

## Postprint of: *Chemosphere* (186): 968-976 (2017)

1 Novel energy crops for Mediterranean contaminated lands: valorization of  
2 *Dittrichia viscosa* and *Silybum marianum* biomass by pyrolysis

3

4 María T. Domínguez<sup>1, 2\*</sup>, Paula Madejón<sup>1</sup>, Engracia Madejón<sup>1</sup>, Manuel J. Diaz-Blanco<sup>3</sup>

5 <sup>1</sup>Instituto de Recursos Naturales y Agrobiología de Sevilla (IRNAS-CSIC), 10 Reina  
6 Mercedes Av. 41012 Seville (Spain)

7 <sup>2</sup>Departamento de Cristalografía, Mineralogía y Química Agrícola, Universidad de  
8 Sevilla, 1 Prof. García González St. 41012 Seville (Spain).

9 <sup>3</sup>PRO2TECS. Department of Chemical Engineering, Huelva University, 21071 Huelva,  
10 Spain

11 \*Corresponding author: [maitedn@irnase.csic.es](mailto:maitedn@irnase.csic.es)

12

### 13 **Abstract**

14

15 Establishing energy crops could be a cost-efficient alternative towards the valorization  
16 of the plant biomass produced in contaminated lands, where they would not compete  
17 with food production for land use. *Dittrichia viscosa* and *Silybum marianum* are two  
18 native Mediterranean species recently identified as potential energy crops for degraded  
19 lands. Here, we present the first characterization of the decomposition of the biomass of  
20 these species during thermo-chemical conversion (pyrolysis). Using a greenhouse study  
21 we evaluated whether the quality of *D. viscosa* and *S. marianum* biomass for energy  
22 production through pyrolysis could be substantially influenced by the presence of high  
23 concentrations of soluble trace element concentrations in the growing substrate. For  
24 each species, biomass produced in two different soil types (with contrasted trace  
25 element concentrations and pH) had similar elemental composition. Behavior during

26 thermal decomposition, activation energies and concentrations of pyrolysis gases were  
27 also similar between both types of soils. Average activation energy values were 295 and  
28 300 kJ mol<sup>-1</sup> (for a conversion value of  $\alpha=0.5$ ) for *S. marianum* and *D. viscosa*,  
29 respectively. Results suggest that there were no major effects of soil growing conditions  
30 on the properties of the biomass as raw material for pyrolysis, and confirm the interest  
31 of these species as energy crops for Mediterranean contaminated lands.

32

33 **Keywords:** biofuel; soil remediation; raw material; TGA

34

### 35 **Highlights**

- 36 ● *Dittrichia viscosa* and *Silybum marianum* are promising energy crops for  
37 contaminated lands
- 38 ● Biomass obtained from two contaminated soils was examined during pyrolysis
- 39 ● TGA curves were similar across materials obtained from both soils
- 40 ● Biomass chemical composition and concentrations of pyrolysis gases were also  
41 similar
- 42 ● Results confirm the interest of both species as energy crops for contaminated  
43 lands

44

45

46

47

48

49

50

51 **Novel energy crops for Mediterranean contaminated lands: valorization of**  
52 ***Dittrichia viscosa* and *Silybum marianun* biomass by pyrolysis**

53

54 María T. Domínguez, Paula Madejón, Engracia Madejón, Manuel J. Diaz

55

56 **1. Introduction**

57

58 The establishment of a plant cover in contaminated lands is critical to improve soil  
59 quality and to reduce the spread of contaminants through soil erosion (Mendez and  
60 Maier, 2008). However, accumulation of contaminants into aboveground biomass often  
61 prevents the agricultural use of these lands (Madejón et al., 2009). Establishing energy  
62 crops could be an alternative towards the valorization of the plant biomass produced in  
63 contaminated lands (Ruttens, 2011; Witters et al., 2012). These crops would not  
64 compete with food production for land use in these marginal areas, and would  
65 contribute to the attainment of national renewable energy targets.

66

67 Due to a long history of mining activities in the Mediterranean Basin, trace-element  
68 (TE) contaminated lands are frequent in Mediterranean countries. Extraction and  
69 processing of metals have resulted in vast extensions of land where wastes have been  
70 deposited and left abandoned, posing a serious threat to environment and local  
71 populations in this region (Doumas et al., 2016). Achieving the remediation of these  
72 contaminated sites will likely be an obligation for EU Member States in the upcoming  
73 years, if the European Soil Framework Directive is finally approved (European  
74 Commission, 2006). The use of energy crops in TE contaminated lands would pose an  
75 opportunity to generate an added-value product from these degraded sites in

76 Mediterranean countries.  
77  
78 Many of the most common energy crops, however, have high water requirements and  
79 are not suitable for degraded Mediterranean areas. Therefore, there is a necessity to  
80 explore native plant species with potential as energy crops for this region. Ideally, these  
81 species should: i) be able to tolerate high concentrations of TE in soils; ii) produce high  
82 biomass even in nutrient-poor and physically altered soils; and iii) have a valuable  
83 biomass, in terms of energy value, that can be handled through the whole process from  
84 biomass harvest to biofuel obtainment with low energy inputs. Both the shrub *Dittrichia*  
85 *viscosa* (L.) Greuter and milk thistle *Silybum marianum* (L.) Gaertn. comply with some  
86 of these criteria, and have been recently identified as promising bioenergy crop species  
87 for Mediterranean lands (Robledo and Correal, 2013). These species might have a  
88 particular interest for contaminated sites, given their ability to colonize soils with high  
89 concentrations of TE where other plant species fail to establish (Brunetti et al., 2009;  
90 Martínez-Sánchez et al., 2012).  
91  
92 Previously, we experimentally showed that *D. viscosa* has the ability to produce a high  
93 biomass in highly degraded soils, including extremely acid and TE-contaminated soils,  
94 and that this biomass has a relatively high calorific value, similar to that of other  
95 common bioenergy crops such as *Arundo donax* and *Miscanthus x giganteus*  
96 (Domínguez et al., 2017). This study also found that biomass production of *S.*  
97 *marianum* was less affected by soil contamination than production of *Cynara*  
98 *cardunculus*, another thistle species with a well-known potential as bioenergy crop for  
99 Mediterranean lands (Fernandez et al., 2006), and that the calorific value of *S.*  
100 *marianum* biomass was not influenced by soil contamination. The behavior of *D.*

101 *viscosa* and *S. marianum* biomass during energy conversion processes, however, is still  
102 to be characterized.

103

104 Main technologies for thermo-chemical conversion of biomass include combustion,  
105 gasification and pyrolysis (McKendry, 2002). Pyrolysis presents some advantages over  
106 combustion and gasification, such as the relatively lower temperature requirements, the  
107 lack of oxygen requirement, and the possibility to obtain liquid bio-oil (Bridgwater et  
108 al., 2001). The syngas resulting from pyrolysis, once cleaned, can be used for different  
109 purposes such as gas turbines, fuel cells, synthesis of liquid fuels like methanol, or  
110 chemicals (Yang et al., 2006). In addition, generation of biochar is obtained during  
111 pyrolysis of biomass, which has been shown to have an increasing range of applications  
112 in the agriculture and forestry sectors (reviewed in Kuppusamy et al., 2016). For these  
113 reasons, pyrolysis is often considered as a practical and effective way of producing  
114 bioenergy from raw lignocellulosic materials or biowaste with reduced emissions of  
115 greenhouse gases (Ferreira et al., 2016).

116

117 Understanding pyrolysis kinetics of a raw material is important to predict the  
118 conversion processes and to optimize the design of reactors (Di Blasi, 2008; Van de  
119 Velden, 2010). Thermogravimetric analysis (TGA) is frequently applied to investigate  
120 pyrolytic kinetics of lignocellulosic biomass (Chen et al., 2015; Damartzis et al., 2011;  
121 Ferreira et al., 2016). Analysis of gases evolved during the pyrolysis is also crucial for a  
122 full characterization of the environmental implications of this conversion technology  
123 and of the potential syngas production.

124

125 In this work, we assessed the potential valorization of *D. viscosa* and *S. marianum*

126 biomass produced in TE-contaminated soils through pyrolysis to produce syngas. We  
127 analyzed elemental composition of biomass, pyrolysis kinetics and composition of gases  
128 evolved during the application of this conversion technology, using the biomass  
129 obtained in a greenhouse experiment that aimed to test the sensitivity of these plant  
130 species to soil contamination. With this, we aimed to evaluate whether the quality of *D.*  
131 *viscosa* and *S. marianum* biomass for syngas production through pyrolysis could be  
132 substantially influenced by soil conditions during plant growth. As reported for other  
133 conversion technologies, such as gasification, soil contamination might result in a lower  
134 quality of biomass for biofuel production, by affecting plant chemical composition  
135 (Madejón et al., 2016). Analyzing the behavior of the biomass of these species during  
136 thermo-chemical conversion is essential for a complete characterization of their  
137 potential as bioenergy crops. To our knowledge, this is the first description of a  
138 conversion process applied to *D. viscosa* and *S. marianum* biomass.

139

## 140 **2. Materials and Methods**

141

### 142 2.1. Raw materials

143 The plant biomass used in this study was produced in a greenhouse experiment that  
144 tested the sensitivity of *D. viscosa* and *S. marianum* productivity to soil contamination.  
145 In this experiment *D. viscosa* and *S. marianum* plants were grown on four different soil  
146 types (acid contaminated, neutral contaminated, and two corresponding uncontaminated  
147 soils - acid and neutral-) that were collected from the Guadiamar River Valley (SW  
148 Spain), an area that was contaminated by a large mining accident in 1998 (Fig. 1). Plant  
149 biomass obtained from the most and the least productive soils (the neutral and the acid  
150 contaminated, respectively) were used for this study. Both soil types are classified as

151 fluvisols and had a low organic matter content (< 2 %); pH in the neutral soil was 6.4,  
152 while the other soil was extremely acidic (pH = 3.1), due to the oxidation of sulphides  
153 deposited onto the soil by the mining accident (Domínguez et al., 2016). In this soil  
154 lower pH conditions promoted a higher solubility of TE. Main properties and TE  
155 concentrations of the experimental soils are shown in Appendix, Table A1.  
156  
157 *D. viscosa* and *S. marianum* seeds were germinated in November 2014, in containers  
158 filled with 15 kg of each soil type. Ten seeds were sown in each container for *S.*  
159 *marianum*, while for *D. viscosa* an amount of 0.05 g, equivalent to 60 seeds, was used.  
160 The containers were kept outdoors until March 2015. Then, 8 containers of each  
161 combination of plant and soil type were moved into a greenhouse where the plants were  
162 grown with irrigation. One of the emerged seedlings per container was left, and the rest  
163 removed. As germination rates in the acid soil were very low, an application of sugar  
164 beet lime as soil amendment was conducted to correct soil pH. This resulted in an  
165 increase in soil pH in the top 5 cm that promoted seed germination, but acid soil  
166 conditions remained in lower soil profiles, where most roots developed (Domínguez et  
167 al., 2017). Thus roots were exposed to unfavourable acid conditions during plant growth  
168 in this acid soil treatment. From March to April plants were irrigated twice weekly with  
169 an amount of water equivalent to 4 L m<sup>-2</sup>. In May, due to the increased  
170 evapotranspiration in the greenhouse, sprinkler irrigation was applied, at a dose of 2.8 L  
171 m<sup>-2</sup> day<sup>-1</sup> per container. See Dominguez et al. (2017) for a full description of the  
172 greenhouse experimental design and plant growing conditions over the experiment.  
173  
174 In summer aboveground biomass in each container was harvested and washed with  
175 deionized water, dried at 70 ° C for at least 48 h and ground in a stainless mill to < 1

176 mm, then further milled to  $< 500 \mu\text{m}$  in a ball mill for pyrolysis experiments. Samples  
177 were stored in a small glass bottle to prevent the contact with air moisture. Biomass  
178 samples of three individual plants (grown in individual containers) per soil type and  
179 species were used for all analyses ( $N = 12$ ).

180

## 181 2.2. Elemental composition analysis

182 The determination of contents in C, H, N and S was performed in a LECO TruSpec  
183 CHN elemental analyzer. The oxygen content was calculated by the difference of the  
184 mole fraction. Each sample was analyzed in duplicate. Dry matter content, metal  
185 concentrations in aboveground biomass and gross calorific values were also analyzed as  
186 described in Domínguez et al., (2017) and are reported in Appendix, Table A2.

187

## 188 2.3. Pyrolysis and TGA experiments

189 A laboratory-scale reactor was used to study the gases evolved from pyrolysis of  
190 biomass. The experimental system consisted of a quartz tube, 10 mm wide, where the  
191 sample (approximately 2g,  $< 500 \mu\text{m}$  particle size) is uniformly introduced inside a tube  
192 of 35 cm length. A horizontal actuator introduced the tube with the biomass into a  
193 furnace maintained at  $550^\circ\text{C}$  at constant velocity, and with 2 s of residence time.  
194 Nitrogen ( $20 \text{ cm}^3 \text{ min}^{-1}$ ) was used as transport gas. Hydrogen, CO and  $\text{CO}_2$   
195 determinations were performed by using a previously calibrated multi-gas analyzer  
196 (MultiRAE IR PGM-54, RAE Systems, San José, CA, USA), and were done in  
197 triplicate, using an integrated sampling pump with a flow rate of  $0.2 \text{ L min}^{-1}$ .

198

199 Thermo-chemical decomposition behavior was assessed using a thermo-gravimetric  
200 analyzer (TGA, Mettler Toledo TGA/DSC1 STARe System). The TGA experiments



201 were performed by heating a 50-130 mg sample from 25°C to 800°C at four heating  
202 rates (5, 10, 15 and 20°C min<sup>-1</sup>, respectively) under a nitrogen flow of 20 cm<sup>3</sup> min<sup>-1</sup>.  
203 TGA data were analyzed to determine the Arrhenius activation energy (E<sub>a</sub>) and the pre-  
204 exponential constant (A) using the Flynn-Wall-Ozawa iso-conversion method (see  
205 section 2.4).

206

#### 207 2.4. TGA kinetic analysis

208 Activation energy (E<sub>a</sub>) has been studied with different mathematical methods  
209 (Damartzis et al., 2011; Fernández et al., 2016). Among these, the use of the iso-  
210 conversion method has been successfully documented for pyrolysis kinetics  
211 determination (Mehrabian et al., 2012; El-Sayed et al., 2015). For a single-reaction  
212 mechanism, E<sub>a</sub> should be a constant value throughout the weight loss region. Activation  
213 energy values for the degradation process were determined by the iso-conversional  
214 Flynn-Wall-Ozawa (FWO) method (Flynn and Wall, 1966; Ozawa, 1965) defined by  
215 Eq. 1:

$$216 \ln(\beta) = \ln\left(\frac{A E_a}{R g(\alpha)}\right) - 2.315 - 0.4567 \frac{E_a}{RT} \text{ (Eq 1),}$$

217 where  $\beta$  is the heating rate, A is the pre-exponential factor,  $g(\alpha)$  is a function of the  
218 conversion, E<sub>a</sub> is the activation energy, T is temperature and R is the gas constant.

219 For different heating rates ( $\beta$ ) and a given degree of conversion ( $\alpha$ ), a linear relationship  
220 is observed when plotting the natural logarithm of heating rates ( $\ln \beta$ ) against 1/T.

221 Activation energy can be calculated from the slope of the straight line describing this  
222 relationship (-0.4567 (E<sub>a</sub>/RT)). The underlying assumption is that the reaction model,  
223  $g(\alpha)$ , is identical at a given degree of conversion ( $\alpha$ ) for a given reaction under different  
224 thermal conditions. This method can be used for determination of the E<sub>a</sub> values without  
225 any knowledge of the reaction mechanisms (El-Sayed et al., 2015). Disadvantage of this

226 method is the requirement of a series of measurements at different heating rates, which  
227 must be made with the same samples mass and the same volume flow of inert gas, with  
228 inherent fluctuations that can be source of errors (Opfermann, et al., 2002). In this study  
229 four replicates of each material were tested to prevent these errors.

230

### 231 2.5. Data analysis

232 For each species, differences in the elemental composition of the biomass obtained from  
233 the two types of soils were explored by applying one-way Anova and Duncan's multiple  
234 range tests (three replicates for each species and soil type). Likewise, these analyses  
235 were applied to test for significant differences in the composition of the gas resulting  
236 from pyrolysis, as well as in activation energies for different conversion values. For *S.*  
237 *marianum*, activation energy data did not met the homoscedasticity assumption, and  
238 Kruskal-Wallis tests were applied to analyze differences in  $E_a$  values between samples  
239 with different soil origin. All these analyses were conducted using R 3.3.2.

240

## 241 3. Results and Discussion

242

### 243 3.1. Chemical characterization

244 *D. viscosa* was able to produce a significant amount of biomass in the acid soil ( $24.7 \pm$   
245  $4.2$  g dw plant<sup>-1</sup>; mean  $\pm$  st. error), being comparable to the production in the neutral soil  
246 ( $22.2 \pm 1.5$  g dw plant<sup>-1</sup>), despite that the conditions in the rooting zone of the acid soil  
247 promoted the solubilization of toxic TE in the rhizosphere (Domínguez et al., 2017).  
248 Elemental analysis of a subset of plants grown in these two types of soils revealed that  
249 C, H, N, O and S composition of *D. viscosa* biomass was neither affected by the soil  
250 type (one-way Anova with soil type as categorical factor non-significant, Table 1).

251 Mean values ( $\pm$  std. error, %) were  $41.5 \pm 0.3$  (C),  $5.60 \pm 0.10$  (H),  $1.02 \pm 0.04$  (N),  
252  $51.5 \pm 0.03$  (O) and  $0.33 \pm 0.04$  (S).

253

254 Biomass produced by *S. marianum* was lower than that produced by *D. viscosa*, without  
255 significant differences in production between the two soil types ( $5.24 \pm 1.13$  g dw plant<sup>-1</sup>  
256 and  $6.93 \pm 2.63$  g dw plant<sup>-1</sup> in the neutral and acidic soils, respectively). For this  
257 species there was only a slight difference in the content of S between samples with  
258 different soil origins, being higher in those plants grown in the neutral soil (mean of  
259 0.33 %) than in the acidic soil (mean of 0.32 %). Mean values ( $\pm$  std. error, %) were  
260  $41.9 \pm 0.6$  (C),  $5.71 \pm 0.06$  (H),  $1.32 \pm 0.05$  (N), and  $50.7 \pm 0.06$  (O).

261

262 Both materials had, therefore, similar elemental composition, although the O/C ratio  
263 was higher for *S. marianum*. On average, H/C and O/C ratios were 0.13 and 1.11,  
264 respectively, in *D. viscosa*, and 0.14 and 1.21, respectively, in *S. marianum*. As the O/C  
265 value is closely related to the calorific value of the material (decreasing with increased  
266 O/C ratio; Ferreira et al., 2016), this could explain the higher calorific value of *D.*  
267 *viscosa* ( $17.20$  MJ kg<sup>-1</sup>) in comparison to *S. marianum* biomass ( $16.3$  MJ kg<sup>-1</sup>;  
268 Appendix Table A3). In comparison to other works with different materials, the O/C  
269 ratio of both *D. viscosa* and *S. marianum* biomass was slightly higher than some  
270 agricultural residues from Mediterranean crops, but lower than some industrial residues  
271 that have been proposed as raw material for pyrolysis, in order to promote the  
272 valorization of residues commonly produced in the Mediterranean region (Ferreira et  
273 al., 2016). Regarding the S content, both materials showed very low levels in  
274 comparison with conventional fuels (0.7–4.9%, Gräbner, 2014), which is a positive  
275 feature, as it reduces the risk of forming S compounds with negative environmental

276 implications, such as H<sub>2</sub>S and SO<sub>2</sub>.

277

### 278 3.2. Thermogravimetric analysis of the pyrolysis process

279 The TGA curves show mass losses of the studied materials (mean of the three replicates  
280 per soil type and plant species) over the range of temperature from 27 °C to 800 °C, at  
281 four heating rates (5, 10, 15 and 20 °C min<sup>-1</sup>) under nitrogen atmosphere (Fig. 2). For  
282 both *D. viscosa* and *S. marianum* materials, the TGA curves exhibit the three thermal  
283 degradation zones typical of lignocellulosic biomass samples (Gašparovič et al., 2010;  
284 Giudicianni et al., 2013), related to moisture evaporation, primary decomposition, and  
285 secondary decomposition, respectively. The first zone, from 60 °C to 180 °C, is related  
286 to the extraction of moisture and water adsorbed into samples. The second region (main  
287 decomposition stage) took place in the temperature range from 180 to 570°C, where  
288 hemicellulose and cellulose decomposition occurs (200-400 °C for hemicellulose and  
289 250-380 °C for cellulose; Dantas et al., 2013). As expected, this was the most active  
290 region, where the greatest mass losses were observed. In the third zone (570-800°C)  
291 decomposition rates were low, and possibly attributed to the gasification of the char  
292 formed over the conversion process (Vuthaluru, 2004). In addition, lignin is  
293 decomposed in the range from 180 to 850 °C without characteristic peaks (Van de  
294 Velden et al. (2010), and therefore some of the mass loss in this third region could be  
295 also attributable to lignin decomposition. The TGA curves were rather similar for all the  
296 studied heating rates, although for both plant species residual mass values at 800 °C  
297 were lower at 5 °C min<sup>-1</sup> (< 20 %) than at the other heating rates (≈ 25 %), possibly  
298 indicating a greater volatilization of biomass at a low heating rate. Similar residual mass  
299 values at 800 °C have been obtained in the pyrolysis of different biomass samples, such  
300 as Camel grass (Mehmood et al., 2016), rice straw (Xu and Chen, 2013) and agricultural

301 residues such as walnut shells and olive waste from olive oil production (Ferreira et al.,  
302 2016). For each species, TGA curves obtained from samples with different soil origins  
303 were rather similar (Fig. 2).

304

305 Inspection of derivative thermogravimetric (DTG) curves confirmed that, for each  
306 species, biomass produced in both types of soils had a similar behavior during thermal  
307 degradation (Fig. 3). For both *D. viscosa* and *S. marianum* the peak of maximum  
308 thermal decomposition was observed at  $\approx 350$  °C, with maximum weight loss rates  
309 around 9 % min<sup>-1</sup> at a heating rate of 20 °C min<sup>-1</sup>. As mentioned above, heating rates  
310 had a modest effect on the dynamics of thermal decomposition, so that decomposition  
311 peaks occurred at similar temperatures under all the tested heating rates. However,  
312 shoulder peaks occurred in the region of hemicellulose degradation (180-350 °C; Dantas  
313 et al., 2013) at high heating rates (< 15-20 °C min<sup>-1</sup>), especially in *D. viscosa* samples.  
314 According to Gaur and Reed (1998), these shoulder peaks could be due to the  
315 interaction among wood biomass polymers (cellulose, hemicellulose and lignin); within  
316 the range of 150 -180 °C the stability of cellulose is reduced, and it might react with  
317 hemicelluloses, while at greater temperatures (300°C to 400°C) cellulose decomposes  
318 quickly (Stefanidis et al., 2013), with a large decomposition peak. Flat tailing sections  
319 were observed in the DTG curves at the range of 400 °C to 750 °C, likely associated to  
320 lignin decomposition, which is known to decompose slowly over a broad temperature  
321 range. Small decomposition peaks were observed at 800 °C, being higher in *S.*  
322 *marianum* than in *D. viscosa* samples, likely revealing differences in the amount of  
323 lignin between the two types of biomass.

324

325 3.3. Analysis of pyrolysis kinetics

326 Kinetic parameters were calculated according to Eq. (1) at three conversion ( $\alpha$ ) values  
327 (0.25, 0.5 to 0.75) for all curves (different heating rates), following the FWO method.  
328 The FWO equations (slope and  $R^2$ ) describing the relationship between  $\ln(\beta_i)$  and  $1/T_{oi}$ ,  
329 as well as apparent activation energy ( $E_a$ ) values calculated from the slopes of these  
330 equations (individual samples) are shown in Appendix Tables A3 and A4.

331

332 In general, the calculated  $E_a$  values at the different conversion rates were similar for  
333 both *D. viscosa* and *S. marianum* (Table 2). With the exception of one *S. marianum*  
334 sample,  $R^2$  values were  $> 0.93$  at all conversion rates. The obtained  $E_a$  values were  
335 highly dependent on the extent of conversion, which could indicate that the pyrolysis  
336 process in these materials is a multi-step reaction and not a single reaction mechanism  
337 (Sonobe and Worasuwannarak, 2008). As with elemental composition, there were not  
338 significant differences in  $E_a$  values between biomass samples obtained from different  
339 soils at any conversion rate (Table 1).

340

341 At low conversion ( $\alpha < 0.25$ ), which corresponds to the thermal degradation of the  
342 hemicellulose and the beginning of cellulose degradation (Nada and Hassan, 2000),  $E_a$   
343 varied between 126 and 171  $\text{kJ mol}^{-1}$  in the samples of both plant species. In  
344 comparison with published data on  $E_a$ , slightly higher  $E_a$  values (213  $\text{kJ mol}^{-1}$ ) have  
345 been reported by Lv et al., (2010) for hemicellulose activation energy, using the same  
346 kinetic method. Cellulose activation energy is usually reported to be greater than  
347 hemicellulose  $E_a$  (Gašparovič et al., 2010), with reported values ranging between 178.7  
348  $\text{kJ mol}^{-1}$  (Saddawi et al., 2010) and 226  $\text{kJ mol}^{-1}$  (Lin et al., 2013), while lignin  
349 activation energy has been reported in the range of 237.1-266.6  $\text{kJ mol}^{-1}$  under  
350 isothermal heating conditions (Junmeng et al., 2013). Maximum  $E_a$  values in this study

351 were observed at  $\alpha=0.5$ , ranging from 273 to 429.4 kJ mol<sup>-1</sup> in *D. viscosa* (average  
352 around 300 kJ mol<sup>-1</sup>), and from 204 to 370 kJ mol<sup>-1</sup> in *S. marianum* (average around 295  
353 kJ mol<sup>-1</sup>). Activation energies between 118.8 and 150.9 kJ mol<sup>-1</sup> in *D. viscosa*, and  
354 between 101 and 151 kJ mol<sup>-1</sup> in *S. marianum* were found for  $\alpha=0.75$ .

355

356 In comparison to previously reported  $E_a$  values, calculated  $E_a$  of *D. viscosa* and *S.*  
357 *marianum* ( $\alpha=0.5$ ) were found to be higher than other common raw materials, such as  
358 Miscanthus (113–143 kJ mol<sup>-1</sup>; Cortés and Bridgwater, 2015), *Eucaliptus grandis* (218  
359 kJ mol<sup>-1</sup>; Poletto et al., 2012) or poplar (198 kJ mol<sup>-1</sup>; Słopiecka et al., 2011). The  
360 similar  $E_a$  of both *D. viscosa* and *S. marianum* biomass suggest that these two raw  
361 materials could be pyrolyzed together; likewise other common raw materials with lower  
362  $E_a$  could be used for co-firing with *D. viscosa* or *S. marianum* biomass.

363

#### 364 3.4 Gases obtained during pyrolysis

365 The concentrations of gases (CO, CO<sub>2</sub> and H<sub>2</sub>) obtained during pyrolysis of *D. viscosa*  
366 and *S. marianum* biomass are shown in Table 3. Although the composition of syngas  
367 depends on the biomass properties and gasifier operating conditions (Basu, 2013), under  
368 fixed conditions obtained data may be useful for comparison among different  
369 treatments. In relation to our treatment (different soil types in the growing substrate),  
370 slightly higher H<sub>2</sub> values were found for some samples of *D. viscosa* produced in the  
371 neutral soil, although differences with the pyrolysis gases of those samples produced in  
372 the acid soil were not statistically significant (Table 1). For *S. marianum*, differences in  
373 pyrolysis gases between soil types were neither observed (Table 1). We could have  
374 expected a significant increase in H<sub>2</sub> concentrations in the gas obtained from biomass  
375 produced in the neutral soil (more favorable for plant growth), as found in a previous

376 work with *Paulownia fortuneii* biomass obtained from the same experimental soils  
377 (Madejón et al., 2016). However, in that work differences in plant growth and status  
378 between soil types were larger than those detected for *D. viscosa* and *S. marianum* in  
379 this study.

380

381 When  $E_a$  values were compared with the composition of the gas obtained during the  
382 pyrolysis process, a negative relationship between  $H_2$  concentration and  $E_a$  was  
383 observed for  $\alpha=0.5$ , which in most cases corresponded to the maximum activation  
384 energy of the process (Fig. 4). Ideally, optimal features as raw material for pyrolysis  
385 would include a high concentration of  $H_2$  in the resulting syngas and minimal activation  
386 energy required during pyrolysis. All analyzed samples spanned broadly over the curve  
387 describing this  $H_2$ - $E_a$  relationship, without a clear distinction between *D. viscosa* or *S.*  
388 *marianum* samples, or between samples obtained from the different experimental soils.

389 This suggests, together with the similar behavior of biomass decomposition as indicated  
390 by TGA analysis, and with the similar elemental composition of biomass between soil  
391 types, that the properties of *D. viscosa* and *S. marianum* biomass relevant for energy  
392 conversion processes would not be particularly affected by the plant growing  
393 conditions, in particular by acidic soil conditions that promote the availability of toxic  
394 trace elements in the rhizosphere. Although C, H, O, N and S concentrations were not  
395 affected by the soil type, concentrations of some trace elements, particularly Cd,  
396 increased in those plants grown in the acid soil (Domínguez et al., 2017). This issue  
397 should be further evaluated before establishing these species as energy crops in  
398 contaminated lands, given than metal-enriched ash could be produced during energy  
399 conversion processes, which may reduce the environmental sustainability of the  
400 bioenergy crop system.



401

### 402 3.5 Future recommendations

403 The results suggest that the quality of *D. viscosa* and *Silybum marianum* for bioenergy  
404 production through pyrolysis is not severely affected by conditions of acidity and trace  
405 element contamination in the growing substrate. Given the relatively low water  
406 requirements of these species (Ledda et al., 2013; Robledo and Correal, 2013) and their  
407 ability to grow in highly degraded soils (Gómez-Ros et al., 2013; Río-Celestino et al.,  
408 2006), there is a potential for establishing these species as bioenergy crops in  
409 contaminated Mediterranean lands, if adequate soil preparation is accomplished to  
410 reduce the inhibition of seed germination imposed by low pH in acidic soils  
411 (Domínguez et al., 2017). Besides the benefits of lignocellulosic biomass production,  
412 the establishment of these species could promote the recovery of soil quality in the  
413 contaminated lands; short-term effects of *S. marianum* plantation included a stimulation  
414 of soil enzyme activities, possibly due to a high release of exudates by *S. marianum*  
415 roots that could stimulate the activity of its rhizospheric microbial community  
416 (Domínguez et al., 2017). In addition, *D. viscosa* had an ability to develop an extensive  
417 root system shortly after its plantation (Domínguez et al., 2017), which contributes to  
418 the physical stabilization of the soil, thus reducing the risk of spreads of contaminants  
419 through soil erosion.

420

421 Nevertheless, further studies are needed to confirm the suitability of these species for  
422 bioenergy production purposes. Firstly, a complete assessment of the accumulation of  
423 metals into aboveground biomass under field conditions must be conducted, as exposed  
424 above, including an evaluation of potential problems associated to the production of  
425 metal-enriched ash during thermo-chemical conversion. Secondly, a complete

426 characterization of the energy balance during crop establishment and biomass  
427 processing is required to estimate the costs associated to the management of these new  
428 crops. Therefore, longer-term and field-scale experimental studies would be needed to  
429 support the evidences of suitability of these species as energy crops for contaminated  
430 lands. Finally, other technical factors and variables involved in the pyrolysis of biomass  
431 should be analyzed more in detail for a full characterization of these raw materials,  
432 including the production of oil and biochar, as well as the release of tar during the  
433 pyrolysis process.

434

#### 435 **4. Conclusions**

436

437 Biomass of *Dittrichia viscosa* and *Silybum marianum* produced in two different  
438 contaminated Mediterranean soils (with contrasted trace element concentrations and  
439 acidity conditions) had similar elemental composition. TGA curves revealed similar  
440 peaks of decomposition (with a maximum at  $\approx 350$  °C) in both species. In addition,  $E_a$   
441 values were similar in both types of biomass. For each plant species TGA curves were  
442 similar in samples obtained from both types of soils, as well as concentrations of  
443 pyrolysis gases (CO, CO<sub>2</sub> and H<sub>2</sub>). These results suggest that there were no major  
444 effects of the soil growing conditions on the properties of the biomass as raw material  
445 for pyrolysis. A complete characterization of the energy balance during crop  
446 establishment and biomass processing, as well as an evaluation of potential problems  
447 associated to the production of metal-enriched ash during thermos-chemical conversion  
448 would be needed to confirm the suitability as energy crop species for TE-contaminated  
449 lands in the Mediterranean region.

450

451 **5. Acknowledgements**

452

453 This work was supported by the Iberdrola Foundation (Young Researchers Program) and  
454 the Spanish Ministry of Economy and Competitiveness (AGL2014-55717-R project and  
455 CTQ2013-46804-C2-1-R projects). We are grateful to Patricia Puente and Cristina  
456 García for their help at different stages of the study. MTD was supported by a Juan de la  
457 Cierva Postdoctoral fellowship from the Spanish Ministry of Economy and  
458 Competitiveness, and a postdoctoral fellowship from University of Seville (V Plan  
459 Propio).

460

461 **6. References**

462

- 463 Basu P. Biomass co-firing and torrefaction. In: Basu P, editor. Biomass gasification,  
464 pyrolysis and torrefaction, Amsterdam: Elsevier; 2013, p. 353–373.
- 465 Bridgwater AV, Czernik S, Piskorz J. An Overview of Fast Pyrolysis. In: Bridgwater  
466 AV, editor. Progress in thermochemical biomass conversion, Oxford: Blackwell  
467 Science Ltd; 2001, p. 977–997.
- 468 Brunetti G, Soler-Rovira P, Farrag K, Senesi N. Tolerance and accumulation of heavy  
469 metals by wild plant species grown in contaminated soils in Apulia region,  
470 Southern Italy. *Plant Soil* 2009; 318: 285–298.
- 471 Chen C, Miao W, Zhou C, Wu H. Thermogravimetric pyrolysis kinetics of bamboo  
472 waste via Asymmetric Double Sigmoidal (Asym2sig) function deconvolution.  
473 *Bioresour Technol* 2017; 225: 48–57.
- 474 Cortés AM, Bridgwater A. Kinetic study of the pyrolysis of miscanthus and its acid  
475 hydrolysis residue by thermogravimetric analysis. *Fuel Process Technol* 2015;

476 138: 184–193.

477 Damartzis T, Vamvuka D, Sfakiotakis S, Zabaniotou A. Thermal degradation studies  
478 and kinetic modeling of cardoon (*Cynara cardunculus*) pyrolysis using  
479 thermogravimetric analysis (TGA). *Bioresour Technol* 2011; 102: 6230–6238.

480 Dantas, G. A., Legey, L. F., Mazzone, A. Energy from sugarcane bagasse in Brazil: An  
481 assessment of the productivity and cost of different technological routes. *Renew.*  
482 *Sust. Energ. Rev.* 2013; 21: 356–364.

483 Di Blasi C. Modeling chemical and physical processes of wood and biomass pyrolysis.  
484 *Prog Energy Combust Sci* 2008; 34: 47–90.

485 Domínguez MT, Alegre J, Madejón P, Madejón E, Burgos P, Cabrera F, Marañón T,  
486 Murillo J M. River banks and channels as hotspots of soil pollution after large-  
487 scale remediation of a river basin. *Geoderma* 2016; 261: 133–140.

488 Domínguez MT, Montiel-Rozas MM, Madejón P, Diaz MJ, Madejón E. The potential  
489 of native species as bioenergy crops on trace-element contaminated  
490 Mediterranean lands. *Sci Total Environ* 2017; 590–591: 29–39.

491 Doumas P, Munoz M, Banni M, Becerra S, Bruneel O, Casiot C, Cleyet-Marel J-C,  
492 Gardon J, Noack Y, Sappin-Didier V. Polymetallic pollution from abandoned  
493 mines in Mediterranean regions: a multidisciplinary approach to environmental  
494 risks. *Reg Environ Change* 2016. doi:10.1007/s10113-016-0939-x

495 El-Sayed SA, Mostafa ME. Kinetic parameters determination of biomass pyrolysis fuels  
496 using TGA and DTA techniques. *Waste Biomass Valori* 2015; 6: 401–415.

497 European Commission. Proposal for a Directive of the European Parliament and of the  
498 Council establishing a framework for the protection of soil and amending  
499 Directive 2004/35/EC /\* COM/2006/0232 final - COD 2006/0086 \* 2006.  
500 <http://eur-lex.europa.eu/legal->

501 content/EN/TXT/HTML/?uri=CELEX:52006PC0232&from=EN). [accessed:  
502 14.12. 16].

503 Fernández A, Saffe A, Pereyra R, Mazza G, Rodriguez R. Kinetic study of regional  
504 agro-industrial wastes pyrolysis using non-isothermal TGA analysis. Appl  
505 Therm Eng 2016; 106: 1157–1164.

506 Fernández J, Curt MD, Aguado PL. Industrial applications of *Cynara cardunculus* L.  
507 for energy and other uses. Ind Crops Prod 2006; 24: 222–229.

508 Ferreira C I, Calisto V, Cuerda-Correa EM, Otero M, Nadais H, Esteves V I.  
509 Comparative valorisation of agricultural and industrial biowastes by combustion  
510 and pyrolysis. Bioresour Technol 2016; 218: 918–925.

511 Flynn J H, Wall LA. General treatment of the thermogravimetry of polymers. J Res Nat  
512 Bu. Stand 1966; 70A: 487.

513 Gašparovič L, Koreňová Z, Jelemenský Ľ. Kinetic study of wood chips decomposition  
514 by TGA. Chem Pap 2010; 64: 174–181.

515 Gaur S, Reed TB. Thermal data for natural and synthetic fuels. New York: Marcel  
516 Dekker; 1998.

517 Giudicianni P, Cardone G, Ragucci R. Cellulose, hemicellulose and lignin slow steam  
518 pyrolysis: Thermal decomposition of biomass components mixtures. J Anal  
519 Appl Pyrolysis 2013; 100: 213–222.

520 Gómez-Ros, J.M., Garcia, G., Peñas, J.M. Assessment of restoration success of former  
521 metal mining areas after 30 years in a highly polluted Mediterranean mining  
522 area: Cartagena-La Unión. Ecol. Eng. 2013; 57: 393–402.

523 Gräbner M. Coal characterization for gasification. In: Gräbner M, editor. Industrial coal  
524 gasification technologies covering baseline and high-ash coal, Weinheim:  
525 Wiley-VCH Verlag GmbH & Co; 2014, p. 25–106.

526 Hanif MU, Capareda SC, Iqbal H, Arazo RO, Baig MA. Effects of pyrolysis  
527 temperature on product yields and energy recovery from co-feeding of cotton gin  
528 trash, cow manure, and microalgae: A simulation study. Plos One 2016; 11:  
529 e0152230 doi:10.1371/journal.pone.0152230

530 Junmeng C, Wu W, Liu R, Huber G W. A distributed activation energy model for the  
531 pyrolysis of lignocellulosic biomass. Green Chem 2013; 15: 1331-1340.

532 Kuppusamy S, Thavamani P, Megharaj M, Venkateswarlu, K, Naidu R. Agronomic and  
533 remedial benefits and risks of applying biochar to soil: Current knowledge and  
534 future research directions. Environ Int 2016; 87: 1–12.

535 Ledda, L., Deligios, P.A., Farci, R., Sulas, L. Biomass supply for energetic purposes  
536 from some Cardueae species grown in Mediterranean farming systems. Ind.  
537 Crops Prod. 2013; 47: 218–226.

538 Lin T, Goos E, Riedel U. A sectional approach for biomass: Modelling the pyrolysis of  
539 cellulose. Fuel Process Technol 2013; 115: 246–253.

540 Lv G, Wu SB, Lou R. Kinetic study of the thermal decomposition of hemicellulose  
541 isolated from corn stalk. BioResources 2010; 5: 1281-1291.

542 Madejón P, Domínguez MT, Díaz MJ, Madejón E. Improving sustainability in the  
543 remediation of contaminated soils by the use of compost and energy valorization  
544 by *Paulownia fortunei*. Sci Total Environ 2016. 539: 401–409.

545 Madejón P, Domínguez MT, Murillo JM. Evaluation of pastures for horses grazing on  
546 soils polluted by trace elements. Ecotoxicology 2009; 18: 417–428.  
547 doi:10.1007/s10646-009-0296-3.

548 Martínez-Sánchez MJ, García-Lorenzo ML, Pérez-Sirvent C, Bech J. Trace element  
549 accumulation in plants from an aridic area affected by mining activities. J  
550 Geochem Expl 2012; 123: 8–12.

551 Mckendry P. Energy production from biomass (part 2): conversion technologies.  
552 Bioresour Technol 2002; 83: 47–54.

553 Mehmood MA, Ye G, Luo H, Liu C, Malik S, Afzal I, Xu J, Ahmad MS. Pyrolysis and  
554 kinetic analyses of Camel grass (*Cymbopogon schoenanthus*) for bioenergy.  
555 Bioresour Technol 2017; 228: 18–24.

556 Mehrabian R, Scharler R, Obernberger I. Effects of pyrolysis conditions on the heating  
557 rate in biomass particles and applicability of TGA kinetic parameters in particle  
558 thermal conversion modelling. Fuel 2012; 93: 567–575.

559 Mendez MO, Maier RM. Phytostabilization of Mine Tailings in Arid and Semiarid  
560 Environments—An Emerging Remediation Technology. Environ Health Persp  
561 2007; 116: 278–283.

562 Nada A, Hassan ML. Thermal behavior of cellulose and some cellulose derivatives.  
563 Polym Degrad Stabil 2000; 67: 111–115.

564 Opfermann J, Kaisersberger E, Flammersheim H. Model-free analysis of  
565 thermoanalytical data—advantages and limitations. Thermochim Acta 2002; 391:  
566 119–127.

567 Ozawa T. A new method of analyzing thermogravimetric data. Bull Chem Soc Jpn  
568 1965; 38: 1881–1886.

569 Poletto M, Zattera AJ, Santana RMC. Thermal decomposition of wood: Kinetics and  
570 degradation mechanisms. Bioresour Technol 2012; 126: 7–12.

571 Ríó-Celestino, M., Font, R., Moreno-Rojas, R., Haro-Bailón, A. Uptake of lead and zinc  
572 by wild plants growing on contaminated soils. Ind. Crops Prod. 2006; 24: 230–  
573 237.

574 Robledo A, Correal E. Cultivos energéticos de segunda generación para la producción  
575 de biomasa lignocelulósica en tierras de cultivo marginales. Murcia: Instituto

576 Murciano de Investigación y Desarrollo Agrario y Alimentario; 2013

577 Ruttens A, Boulet J, Weyens N, Smeets K, Adriaensen K, Meers E, Slycken SV, Tack  
578 F, Meiresonne L, Thewys T, Witters N, Carleer R, Dupae J, Vangronsveld J.  
579 Short Rotation Coppice Culture of Willows and Poplars as Energy Crops on  
580 Metal Contaminated Agricultural Soils. *Int J Phytoremediation* 2011; 13: 194–  
581 207.

582 Saddawi A, Jones JM, Williams A, Wójtowicz MA. Kinetics of the thermal  
583 decomposition of biomass. *Energy Fuels* 2010; 24: 1274–1282.

584 Slopiecka K, Bartocci P, Fantozzi F. Thermogravimetric analysis and kinetic study of  
585 poplar wood pyrolysis. *Third International Conference on Applied Energy:*  
586 *Perugia, Italy; 2001, p.1687-1698.*

587 Sonobe T, Worasuwanarak N. Kinetic analyses of biomass pyrolysis using the  
588 distributed activation energy model. *Fuel* 2008; 87: 414–421.

589 Stefanidis SD, Kalogiannis, KG, Iliopoulou EF, Michailof CM, Pilavachi PA, Lappas  
590 AA. A study of lignocellulosic biomass pyrolysis via the pyrolysis of cellulose,  
591 hemicellulose and lignin. *J Anal Appl Pyrolysis* 2014; 105: 143–150.

592 Van de Velden M, Baeyens J, Brems A, Janssens B, Dewil R. Fundamentals, kinetics  
593 and endothermicity of the biomass pyrolysis reaction. *Renew Energy* 2010; 35:  
594 232-242.

595 Vuthaluru H B. Investigations into the pyrolytic behaviour of coal/biomass blends using  
596 thermogravimetric analysis. *Bioresour Technol* 2004; 92: 187–195.

597 Witters N, Mendelsohn R, Slycken SV, Weyens N, Schreurs E, Meers E, Tack F,  
598 Carleer R, Vangronsveld J. Phytoremediation, a sustainable remediation  
599 technology? Conclusions from a case study. I: Energy production and carbon  
600 dioxide abatement. *Biomass Bioenerg* 2012; 39: 454–469.



601 Xu Y, Chen B. Investigation of thermodynamic parameters in the pyrolysis conversion  
602 of biomass and manure to biochars using thermogravimetric analysis. *Bioresour*  
603 *Technol* 2013; 146: 485–493.

604 Yang YB, Sharifi VN, Swithenbank J. Biomass and municipal solid wastes.  
605 Substoichiometric conversion of biomass and solid wastes to energy in packed  
606 beds. *Aiche J* 2006; 52: 809-817.

607

608

609

610

611

612

613

614

615

616

617

618

619

620

621 **Figure captions**

622

623 **Fig. 1** Location of the Guadiamar River Valley in SW Spain, where experimental soils  
624 were collected. AC = acid contaminated soil; NC = neutral contaminated soil.

625

626 **Fig. 2** TGA curves at different heating rates (5, 10, 15 and 20 °C min<sup>-1</sup>) of *D. viscosa*  
627 (A, B) and *S. marianum* biomass (C, D), obtained from neutral and acid contaminated  
628 soils.

629

630 **Fig. 3** DTG curves at different heating rates (5, 10, 15 and 20 °C min<sup>-1</sup>) of *D. viscosa*  
631 (A, B) and *S. marianum* biomass (C, D), obtained from neutral and acid contaminated  
632 soils.

633

634 **Fig. 4** Relationship between H<sub>2</sub> concentration in pyrolysis gases and activation energy  
635 (E<sub>a</sub>) calculated for a conversion value (α) of 0.5 in the analyzed materials. Samples  
636 represented by grey and white symbols correspond to biomass obtained from acid and  
637 neutral contaminated soils, respectively.

638

639

640

641

642

643

644

645

646 **Tables**

647

648 **Table 1** Results of the one-way Anova tests applied to *D. viscosa* and *S. marianum*  
 649 biomass chemical composition, activation energy (at a conversion factor of  
 650  $\alpha = 0.05$ ) and composition of pyrolysis gases, with soil type as categorical factor. <sup>a</sup> For  
 651 *S. marianum*, activation energy data did not met the homocedasticity assumption, and  
 652 Kruskal-Wallis test was applied to analyze differences in  $E_a$  values between samples  
 653 with different soil origin (chi-square and p-values shown).

654

655

656

657

658

659

660

661

662

663

664

665

666

667

668

669

670

Chemical composition	<i>D. viscosa</i>		<i>S. marianum</i>	
	F	p	F	p
C	2.90	0.163528	2.744	0.172981
H	0.027	0.876595	4.00	0.116189
N	0.9356	0.388192	2.8246	0.168123
S	3.36158	0.140661	2.824650	0.168123
O	0.57	0.493324	2.449	0.192631
Activation energy				
$E_a$	0.28610	0.621082	0.666 <sup>a</sup>	0.414200
Pyrolysis gases				
CO	5	0.101192	2	0.230200
CO <sub>2</sub>	1.13	0.348641	0.46	0.536039
H <sub>2</sub>	1.688	0.263751	0.893	0.398208

671 **Table 2** Activation energies ( $E_a$ ,  $\text{kJ mol}^{-1}$ ) obtained by the analysis of pyrolysis kinetics  
 672 ( $\ln(\beta_i)$  vs.  $1/T_{ai}$ , FWO method), at different values of conversion ( $\alpha$ ). Mean  $\pm$  standard  
 673 error for each species and soil type.

	<i>D. viscosa</i>		<i>S. marianum</i>	
	Neutral soil	Acid soil	Neutral soil	Acid soil
676 $\alpha= 0.25$	136.4 $\pm$ 4.9	147.8 $\pm$ 9.4	152.8 $\pm$ 12.5	133.9 $\pm$ 19.7
677 $\alpha= 0.50$	299.5 $\pm$ 41.8	333.7 $\pm$ 48.4	295.2 $\pm$ 39.9	295.1 $\pm$ 11.8
678 $\alpha= 0.75$	120.6 $\pm$ 0.98	132.3 $\pm$ 9.42	117.4 $\pm$ 3.9	126.1 $\pm$ 14.2

679  
680  
681  
682  
683  
684  
685  
686  
687  
688  
689  
690  
691  
692

693 **Table 3** Composition of pyrolysis gases obtained from *D. viscosa* and *S. marianum*  
 694 samples (expressed as volume percentage, %<sub>v</sub>).

695

Gas	Neutral soil		Acid Soil	
	<i>D. viscosa</i>	<i>S. marianum</i>	<i>D. viscosa</i>	<i>S. marianum</i>
CO	24.7 ± 0.1	24.6 ± 0.1	24.8 ± 0.1	24.7 ± 0.1
CO <sub>2</sub>	18.4 ± 0.3	18.5 ± 0.1	18.7 ± 0.1	18.3 ± 0.1
H <sub>2</sub>	8.0 ± 0.2	7.9 ± 0.1	8.1 ± 0.1	7.7 ± 0.1

696

697

698

699

700

701

702

703

704

705

706

707

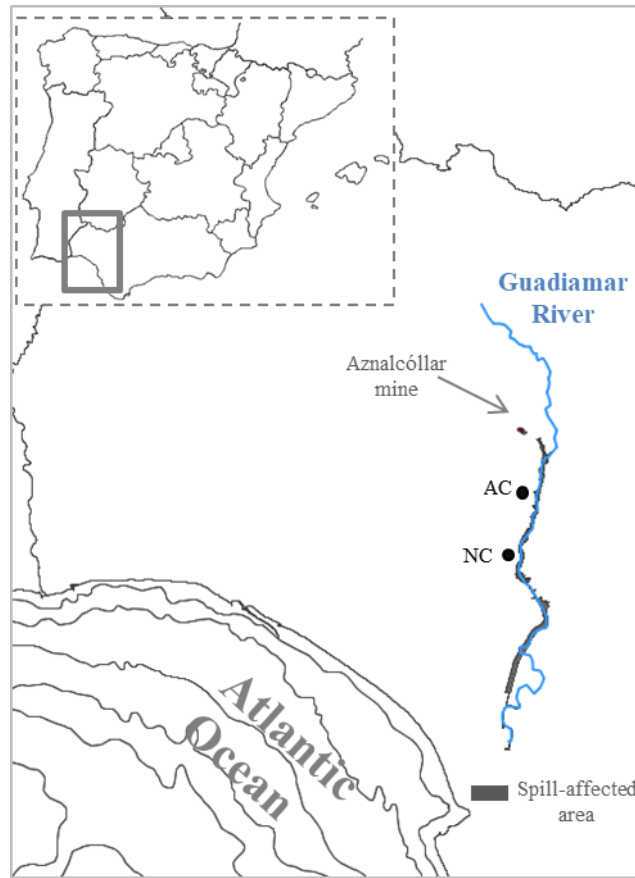
708

709

710

711

712



713

714 **Fig. 1**

715

716

717

718

719

720

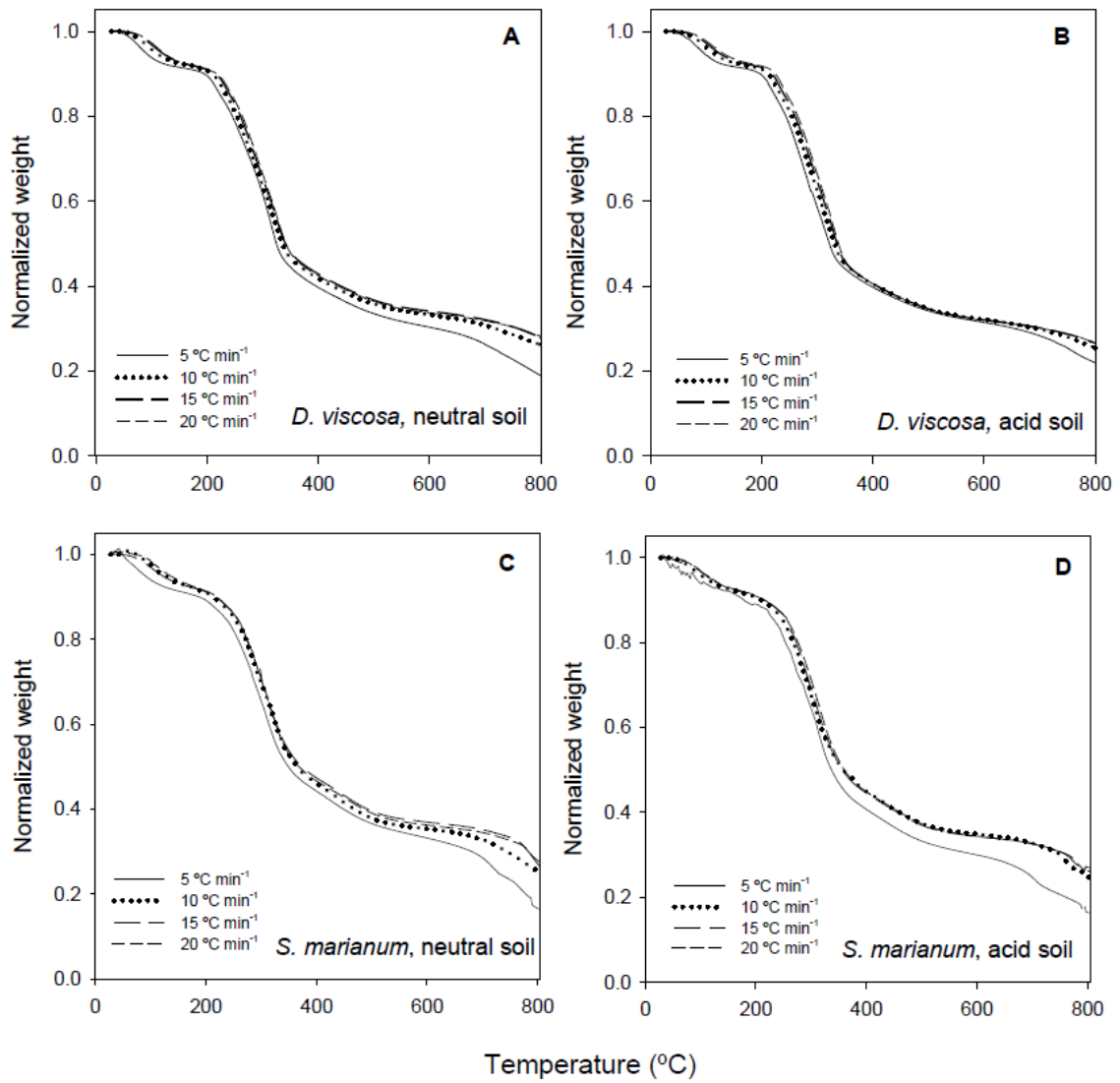
721

722

723

724

725



726

727 **Fig. 2**

728

729

730

731

732

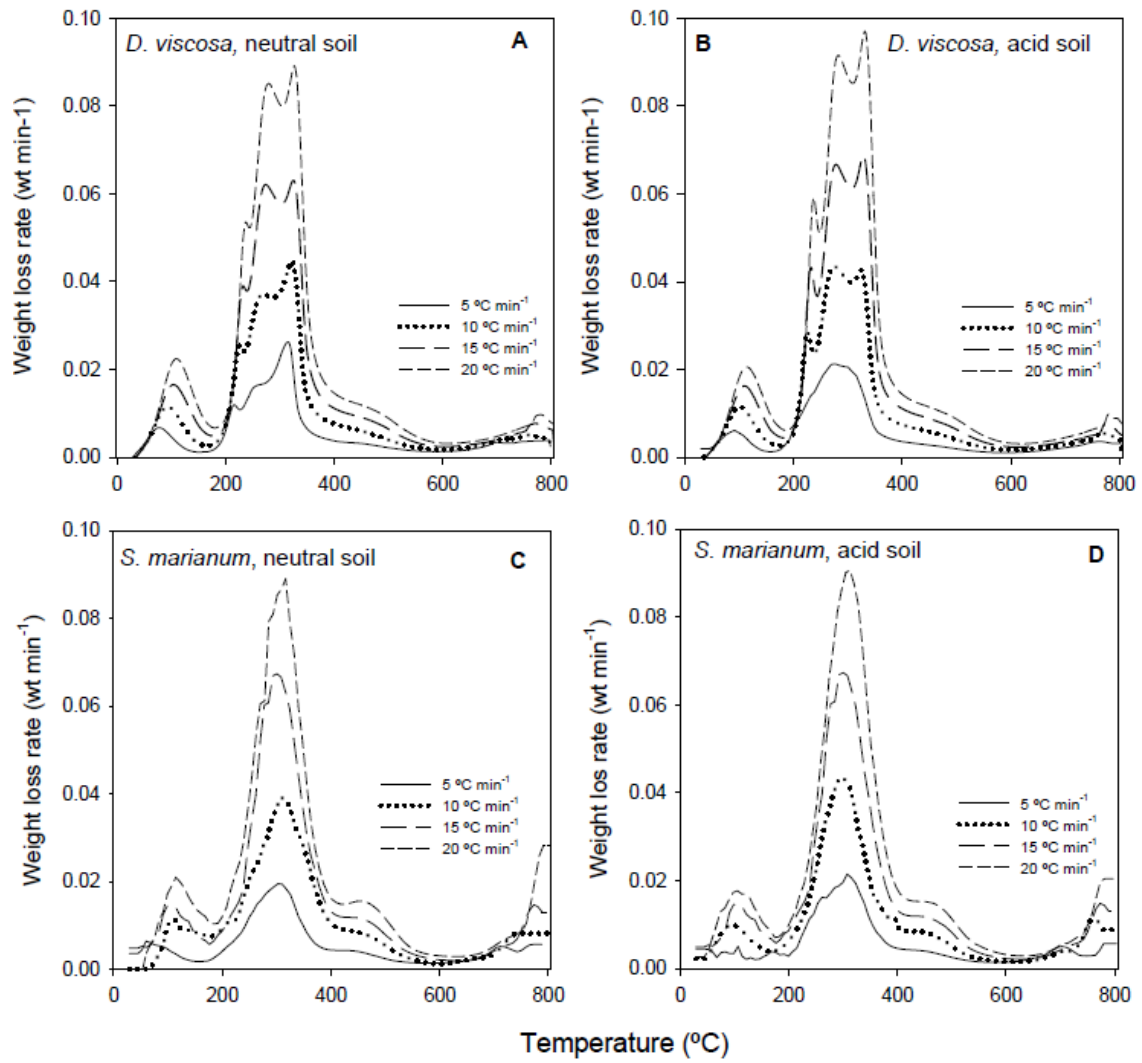
733

734

735

736

737



738

739 **Fig. 3**

740

741

742

743

744

745

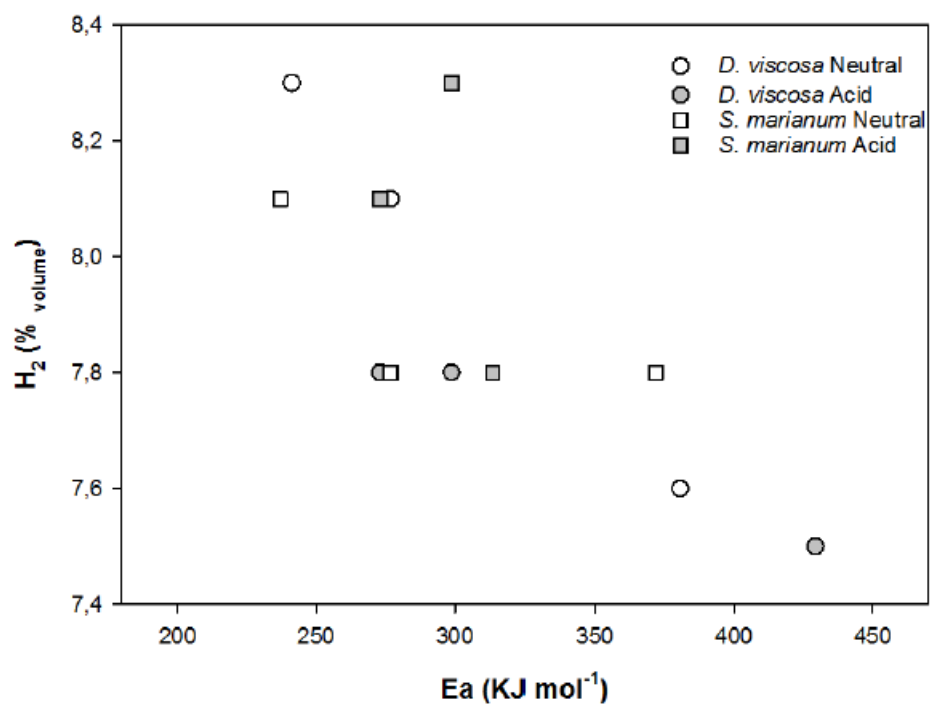
746

747

748

749





750

751 **Fig. 4**